Ion Permeation in Normal and Batrachotoxin-modified Na⁺ Channels in the Squid Giant Axon

ANA M. CORREA, RAMÓN LATORRE, and FRANCISCO BEZANILLA

From the Department of Physiology, Ahmanson Laboratory of Neurobiology and Jerry Lewis Neuromuscular Research Center, University of California, Los Angeles, California 90024; Departamento de Biología, Facultad de Ciencias, Universidad de Chile, Santiago, Chile; Centro de Estudios Científicos de Santiago, Santiago, Chile; and The Marine Biological Laboratory, Woods Hole, Massachusetts 02543

ABSTRACT   Na⁺ permeation through normal and batrachotoxin (BTX)-modified squid axon Na⁺ channels was characterized. Unmodified and toxin-modified Na⁺ channels were studied simultaneously in outside-out membrane patches using the cut-open axon technique. Current–voltage relations for both normal and BTX-modified channels were measured over a wide range of Na⁺ concentrations and voltages. Channel conductance as a function of Na⁺ concentration curves showed that within the range 0.015–1 M Na⁺ the normal channel conductance is 1.7–2.5-fold larger than the BTX-modified conductance. These relations cannot be fitted by a simple Langmuir isotherm. Channel conductance at low concentrations was larger than expected from a Michaelis-Menten behavior. The deviations from the simple case were accounted for by fixed negative charges located in the vicinity of the channel entrances. Fixed negative charges near the pore mouths would have the effect of increasing the local Na⁺ concentration. The results are discussed in terms of energy profiles with three barriers and two sites, taking into consideration the effect of the fixed negative charges. Either single- or multi-ion pore models can account for all the permeation data obtained in both symmetric and asymmetric conditions. In a temperature range of 5–15°C, the estimated Q_{10} for the conductance of the BTX-modified Na⁺ channel was 1.53. BTX appears not to change the Na⁺ channel ion selectivity (for the conditions used) or the surface charge located near the channel entrances.

INTRODUCTION

Batrachotoxin (BTX), a steroidal alkaloid that modifies specifically Na⁺ channels, has been used in the pharmacological and functional characterization of both native and isolated Na⁺ channels (Albuquerque et al., 1973; Catterall, 1975; Rosenberg et al., 1984; Khodorov, 1985; Recio-Pinto et al., 1987; Correa et al., 1990). BTX increases the resting Na⁺ permeability of nerve membranes by removing fast and slow

inactivation and by shifting the voltage-dependent activation toward more hyperpolarized membrane potentials than normal channels (Huang et al., 1982, 1984; Quandt and Narahashi, 1982; Krueger et al., 1983; Moczydlowski et al., 1984).

By eliminating inactivation, BTX allowed the study of native and reconstituted Na^+ channels in lipid bilayer membranes since this toxin induces the appearance of long-lasting openings (Krueger et al., 1983; Hartshorne et al., 1985; Recio-Pinto et al., 1987; Shenkel et al., 1989). In particular, BTX-modified Na^+ channels incorporated in planar lipid bilayers have been used to study the ion conduction properties of a variety of Na^+ channels (Moczydlowski et al., 1984; French et al., 1986a, b; Garber and Miller, 1987; Green et al., 1987; Garber, 1988; Behrens et al., 1989; Naranjo et al., 1989). However, it is not well known what are the main ion conduction changes brought about by the modification of Na^+ channels by BTX. The initial work of Quandt and Narahashi (1982) and Huang et al. (1984) indicates that there is a decrease in channel conductance induced by BTX. This has also been observed for the purified, reconstituted eel Na^+ channel (Shenkel et al., 1989; Correa et al., 1990). On the other hand, Khodorov and Revenko (1979) and Huang et al. (1979) showed that BTX-modified Na^+ channels have a different selectivity than the normal channel (see also Garber and Miller, 1987; Garber, 1988). The ion conduction properties of Na^+ channels appear to vary with the toxin used to diminish or abolish the inactivation process (e.g., Garber and Miller, 1987) and, more dramatically, with the composition of the external and internal media (e.g., Begenisich and Cahalan, 1980a, b; Garber, 1988). However, studies comparing the permeability properties of BTX-modified and normal (unmodified) Na^+ channels in the same preparation are lacking. In this report we study the ion conduction properties of normal and BTX-modified Na^+ channels using the cut-open axon technique (Llano et al., 1988; Bezanilla and Vandenberg, 1990). We found that normal channels have a 1.7–2.5-fold higher conductance than BTX-modified Na^+ channels. In normal and BTX-modified Na^+ channels, the conductance as a function of $[Na^+]$ curves indicates the presence of negative charges in the vicinity of the channel entrances. We describe energy barrier models able to account for the differences in conductance between normal and BTX-modified Na^+ channels. A three-barrier, two-site (3B2S) model comparable to that proposed by Begenisich and Cahalan (1980a, b) for the squid channel was used here. There is enough evidence to believe that inferences regarding ion conduction in normal Na^+ channels from data obtained with toxin-modified channels should be taken with caution.

This work has been reported in preliminary form (Correa and Bezanilla, 1988; Correa et al., 1989).

MATERIALS AND METHODS

Cut-open Axon Technique

The giant axon of the squid *Loligo pealei* was used for these experiments. The procedure to patch clamp the cut-open axon has been described in detail previously (Llano et al., 1988; Bezanilla and Vandenberg, 1990). A summary of the technique follows. A segment of axon of ~1 cm in length, well cleaned of connective tissue, was pinned to the Sylgard-covered (Dow Corning Corp., Midland, Michigan) bottom of the experimental chamber. The axon was then

cut longitudinally (cut-open) with microscissors under artificial seawater (0-K⁺ ASW) containing (in mM): 440 NaCl, 50 MgCl₂, 10 CaCl₂ and 10 HEPES, pH 7.6. The axonal sheet was perfused with ASW to wash out as much of the axoplasm as possible. All experiments reported here were done using the excised outside-out configuration of the patch-clamp technique (Hamill et al., 1981). This configuration was achieved by moving the patch pipette close to the internal surface of the membrane, applying slight suction, and then withdrawing the pipette from the axonal sheet. Unless otherwise indicated, the pipette solution was (in mM): 500 Na-glutamate, 10 NaCl, 20 NaF, and 10 HEPES-NaOH, pH 7.3. Once a high resistance seal was obtained (> 10 GΩ) the external solution was replaced by one containing only Na⁺ as the cation.

Solutions

The different external Na⁺ concentrations were obtained by dilution with 10 mM HEPES of a solution containing (in mM): 540 NaCl and 10 HEPES-NaOH, pH 7.6. Higher Na⁺ concentrations were obtained by increasing the NaCl concentration. Solutions did not contain Ca-chelating agents and the Ca concentration was estimated to be ~ 10 μM at 540 Na and ~ 80 μM at 4 M NaCl. The different internal Na⁺ concentrations were obtained by dilution of the pipette solution with a solution containing (in mM): 5 NaCl, 5 NaF, and 10 HEPES-NaOH. Higher internal Na⁺ concentrations were obtained by increasing the Na-glutamate concentration. The minimum ionic concentration used in the experiments reported here was 15 mM; patches were not stable at lower concentrations. Most experiments were carried out at 5°C. When temperature changes were required, they were varied using Peltier units (Llano et al., 1988).

Channels were modified by adding BTX at a final concentration of 200 nM. Since the appearance of modified channels did not depend on which side the toxin was added to, in the vast majority of the experiments BTX was added to the pipette solution. It was found that the process of modification of Na⁺ channels induced by BTX could be accelerated if the patch was held at hyperpolarized voltages and then depolarized for short periods of time. An alternative way to modify channels was to raise the temperature transiently from 5 to 12–15°C.

Data Acquisition and Analysis

The methodology for pulse generation and data acquisition has been described in detail by Llano et al. (1988). Single-channel currents were stored on a digital tape (Bezanilla, 1985) for subsequent transfer to a digital computer for analysis of channel currents. Before analysis the records were filtered with an eight-pole Bessel filter. Recordings were carefully examined by eye and only events with well-established open levels were used to measure single-channel currents. Two movable horizontal lines placed on top of the traces served as eye markers of baseline and open levels. The difference between the horizontal lines gave the size of the events. Typically, the average of 10–30 determinations at each potential was used for each *I-V* point. However, at extremely positive and negative potentials where the probability of opening and/or closing was less and/or dwell times were shorter, fewer than 10 measurements were frequently obtained. For this reason, in most cases the current vs. voltage curves were constructed with data from several equivalent experiments. *I-V* curves were fitted with a polynomial function, and channel conductance (γ_o) was obtained from the derivative of this function at the origin.

A three-barrier, two-well model was used to calculate the *I-V* relations. To obtain the parameters for the model we used the same strategy as in Cecchi et al. (1986, 1987). A state diagram was drawn, including all the possible connections of the different states of occupancy. Rate constants were stated using the peak and well energies, which are also functions of voltage and electrical distance. A set of steady-state differential equations was written using matrix notation, and the probability of each occupancy state was computed using a matrix inversion

procedure (Hagglund et al., 1984). For convenience, current was computed from the net ion flux across the central barrier,

$$I = e(k_{01}P_{01} - k_{10}P_{10}) \tag{1}$$

where $e = 1.6 \times 10^{-19}$ C/ion, k_{01} and k_{10} are the respective forward and backward rate constants for the ion movement across the central barrier, and P_{01} and P_{10} correspond to the probabilities of occupancy of the external or internal sites of the channel, respectively. Rate constants for the transitions from state i to state j, k_{ij}, are of the form $k_{ij} = (kT/h) \exp [-G_{ij}(V)/kT]$, where $G_{ij}(V)$ is the total energy that the ion needs to overcome to make the transition, and where the transmission coefficient has been taken as unity. T is the temperature in °K, k is Boltzmann's constant, and h is Planck's constant; the frequency factor, kT/h, has units of s^{-1}. On the other hand, for the entry rates (i.e., the steps corresponding to an ion f jumping from the solution into the channel) the kinetic constants are given by $k_{ij} = (kT/h)X_f \exp [-G_{ij}(V)/kT]$, where X_f is a dimensionless mole fraction concentration, computed as the molar ion concentration divided by the molar concentration of water (55.5 M at 20°C) (Eisenman and Dani, 1986). The energies of wells and peaks producing the best fit to the experimental data were found using a nonlinear curve fitting program. Note that for the molar fraction of 1, the reference energy level is taken as $0kT$ (Fig. 8 A); for any concentration other than 55.5 M the difference between the energies of wells and peaks and the reference level will change, whereas those from wells to peaks will remain unaltered.

In order to explain the channel behavior at low [Na$^+$] the channel vestibules are considered to have a net negative charge that gives rise to a potential difference between the channel entrance and the bulk solution. The fixed charge in the vestibule is represented by a planar surface charge density in which one elementary charge per a circle of radius R is assumed. The effect of a fixed charge in the channel entrances was calculated using the Gouy-Chapman double layer theory (e.g., McLaughlin, 1977) and incorporated into the 3B2S model (Villarroel and Eisenman, 1987; Latorre and Alvarez, 1988; Naranjo et al., 1989; Villarroel, 1989). The local concentration C_s is obtained from the relation:

$$C_s = C_b \exp [-eV_s/kT] \tag{2}$$

where C_b is the molar concentration of the ion in the bulk solution and V_s is the surface potential computed from the Gouy-Chapman equation,

$$V_s = (2kT/e) \ln [X + \sqrt{X^2 + 1}] \tag{3}$$

where $X = 136/\pi R^2(C_b)^{1/2}$; here the surface charge density is represented by the term $1/\pi R^2$, which is one elementary charge per surface area defined by a circle with radius R.

One important consequence of the charged-vestibule energy barrier model is that the degree of occupancy of the different kinetic states of the channel is higher at all ion concentrations when compared with a model without surface charge.

RESULTS

Characteristics of Normal and BTX-modified Na$^+$ Channels

Normal channels were studied by pulsing the membrane from a negative holding potential, usually -70 mV, to the different depolarizing voltages. In most experiments several channels were present in the patch (see also Bezanilla, 1987). This fact allowed us to measure channel conductance more precisely, since the larger the amount of channels in the patch, the longer the period of activity before they inactivate. Other factors that helped to measure channel currents accurately were: the

high probability of opening and incomplete fast inactivation of Na^+ channels in the squid axon in the range of positive potentials; multiple reopenings before, and spontaneous return from, inactivation in the range of potentials used; slower kinetics of both fast and slow inactivation at low temperatures; and, finally, the absence of divalent cations that block Na^+ channel currents.

We found that from the several Na^+ channels contained in the patches, very often only one of them was modified by BTX. At the low temperatures used, BTX is less effective than at room temperature. Thus, when required, the process of modification
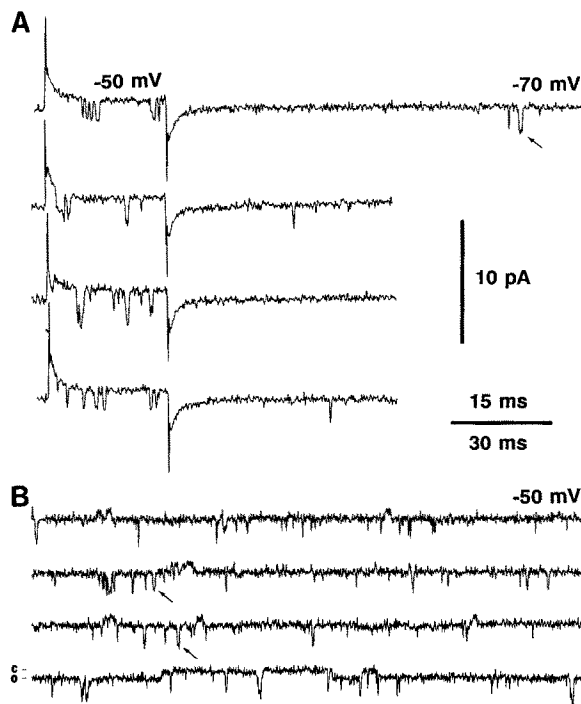

FIGURE 1. (*A*) Current records of normal squid Na^+ channels. The records were obtained from an outside-out patch containing several channels. The potential during the pulses was -50 mV. The holding potential was -70 mV. The small arrow points to a spontaneous opening at the holding potential. (*B*) Current records of normal and BTX-modified Na^+ channels. The traces shown were recorded consecutively during steady depolarization at -50 mV. Openings are downward inflections. Open and closed current levels for the BTX-modified channel are marked by the letters at the beginning of the last trace. The arrows indicate openings of normal (unmodified) channels from the open level of the BTX-modified channel. Data were recorded filtered at 8 kHz bandwidth and digitized for analysis at 20 µs/pt. The records shown were filtered at 2.5 kHz. Recordings were made in symmetrical solutions containing 540 mM external Na^+ and in the presence of 0.2 µM BTX. The time scale bar is 15 ms for records in *A* and 30 ms for those in *B*.

by the toxin was favored through depolarization of the membrane by holding at or pulsing to positive potentials, and/or by warming up the experimental chamber to 15°C. Immediately after the modification of one channel, the chamber was rapidly cooled back to 5°C. The latter strategy helped maintain patches containing a single BTX-modified Na^+ channel for long periods of time (1–2 h). Figs. 1 and 2 show representative records displaying single-channel activity of unmodified and of BTX-modified channels. In Fig. 1 *A* are shown four records exhibiting normal, unmodified Na^+ channel activity at -50 mV during 18-ms pulses. Indicated by the small arrow

below the top trace is a spontaneous opening of a channel at the holding potential of −70 mV. One of the channels in this patch was later modified by BTX. Fig. 1 B shows records obtained at a holding potential of −50 mV after the transformation of such channel. It illustrates the coexistence of several unmodified channels (examples are pointed by the arrows) and a single BTX-modified channel. The closed and open levels of current in the presence of BTX are shown at the beginning of the last trace. Fig. 2 illustrates the process of channel transformation in the same patch. The membrane had been held at −70 mV and sets of pulses to +50, +60, and, finally, +70 mV had been given to favor the conversion. The figure shows the continuous recording right before, during, and after BTX modification, which occurred 8 min
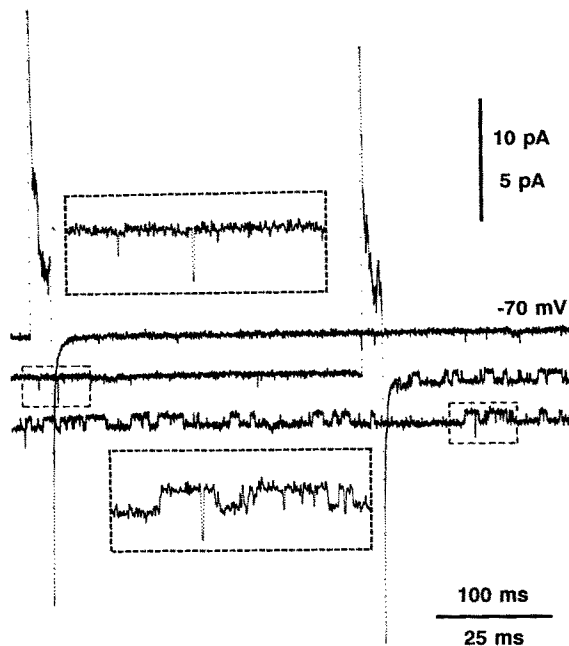
FIGURE 2. Modification of a Na⁺ channel by BTX. The main frame shows a continuous recording at −70 mV (holding potential) with pulses to +70 mV given to promote channel modification. After the second pulse shown here (~8 min after seal formation) a Na⁺ channel is modified by BTX as evidenced by the different kinetics and conductance. The sections of the record enclosed by the rectangles (dashed lines) are expanded in the insets. These display spontaneous openings, from baseline, of unmodified channels before (above) and after (below) the transformation. Recordings are from the same patch as in Fig. 1. For illustration, data were filtered at a 1.5-kHz bandwidth. The smaller values in time and amplitude scales refer to the insets.

after seal formation. The insets show spontaneous openings (from baseline) of normal, unmodified channels. The normal channel also opened from the open level of a BTX-modified channel (see also Fig. 1 B).

As has been determined in many other systems, in the BTX-modified channels of the squid giant axon the voltage-dependent activation curve is shifted toward more hyperpolarized potentials, and the mean open time is much more prolonged than in the normal channel (Correa and Bezanilla, 1988; Correa, A. M., F. Bezanilla, and R. Latorre, manuscript in preparation). The sets of records displayed in Figs. 1 and 2 show that, besides having very different kinetics, normal Na⁺ channels also have a much larger conductance than BTX-modified channels (about twofold in this

particular case). We argue that the larger current openings are in fact unmodified Na$^+$ channels because: (a) They have the same conductance as the ones seen at the same potential during depolarizing pulses (Fig. 1, A and B); (b) Upon depolarization the channels activate and inactivate with kinetics similar to that of macroscopic Na$^+$ currents. Also, the mean open time of the events at potentials between −50 and −20 compare well with the corresponding times of events measured with pulses (Bezanilla, 1987; Vandenberg and Bezanilla, 1988); and (c) These large conductance channels are Na$^+$ selective (see below).
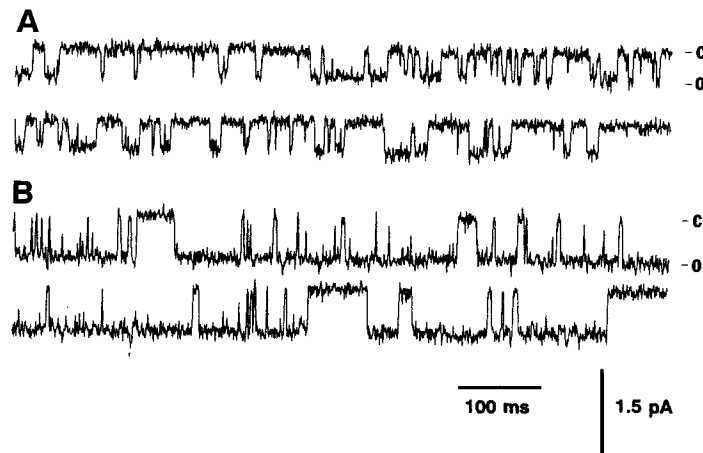

FIGURE 3. BTX-modified Na$^+$ channel current records obtained in the presence of symmetrical solutions containing 15 mM (A) and 540 mM Na$^+$ (B). Voltage, −60 mV. Records filtered at 0.5 kHz.

Conductance–Concentration Relationships

The size of the current jumps at different Na$^+$ concentrations were obtained directly from records like those shown in Figs. 1–3. At each Na$^+$ concentration, current amplitudes were obtained at different membrane potentials and the single-channel I-V relationships were determined. In symmetrical Na$^+$ the I-V relations were fairly linear in the range of potentials studied, although there was a slight tendency to become hyperbolic at [Na$^+$] > 100 mM. Examples of I-V relations at three different concentrations for both normal and BTX-modified channels are shown in Fig. 4. In symmetrical solutions, the conductance at each concentration was determined from the slopes of the I-V relations measured at zero potential (see Methods).

Fig. 5 shows the conductance as a function of Na$^+$ concentration in symmetrical solutions. The conductances for the normal and the BTX-modified Na$^+$ channels are saturating functions of [Na$^+$], but cannot be described by a Michaelis-Menten type of saturation isotherm. Deviations from a simple isotherm at low [Na$^+$] can be explained by considering that there is a fixed negative charge in the vicinity of the channel

entrance(s). The fixed charges located in the neighborhood of the conduction system of the pore create an electrostatic potential, which increases the local concentration of ions. A consequence of this effect is that channel conductance at relatively low ion concentrations is larger than that obtained for the uncharged pore. The solid curves
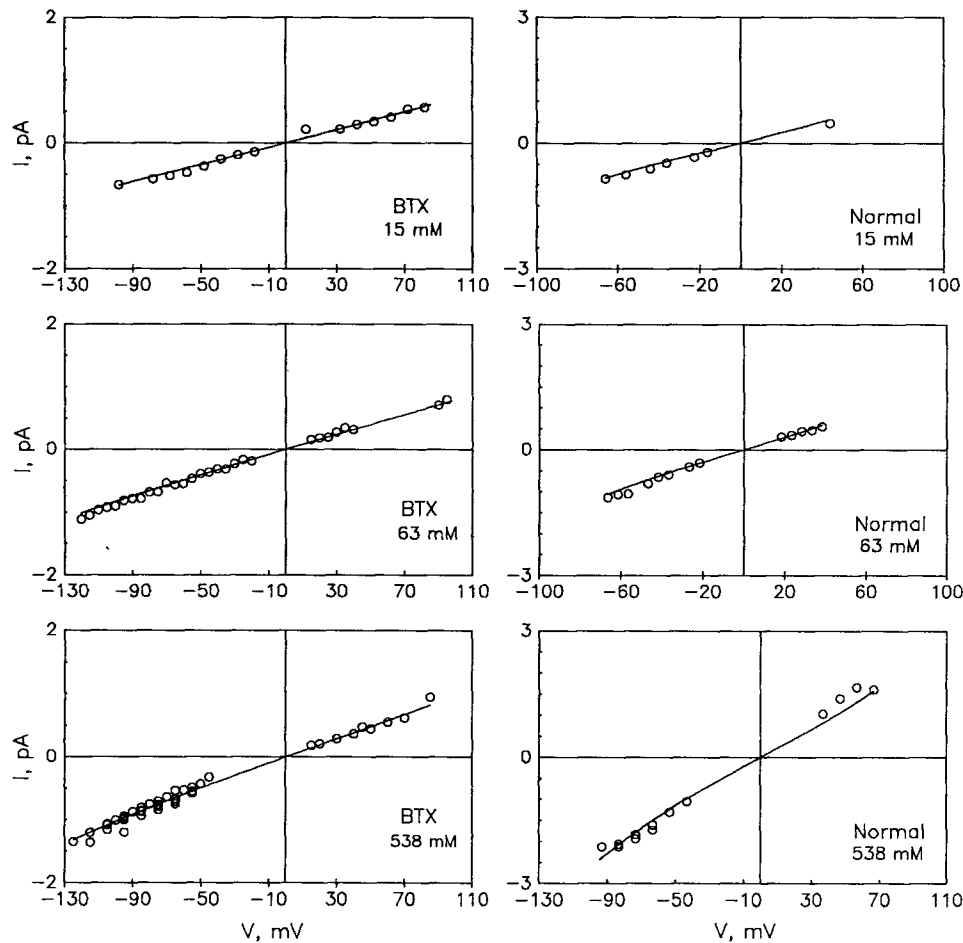

FIGURE 4. *I-V* relationships for BTX-modified (*left panels*) and normal Na$^+$ channels (*right panels*) in symmetrical solutions. Solutions contained Na$^+$ as the only cation at concentrations from 15 to 538 mM. Data at each concentration correspond to separate patches. Note that the current scales are different for normal and BTX-modified Na$^+$ channels. The solid lines are the predicted I-V relationships from the 3B2S barrier model, assuming that the channel vestibules contain a fixed negative charge.

in Figs. 4 and 5 were calculated based on a model assuming a net negative charge, and an energy barrier profile with three barriers and two wells with the proviso that one ion at most can occupy a normal or BTX-modified Na$^+$ channel at any given time (Fig. 8 A). The parameters of the model were obtained by a nonlinear fit of all the *I-V*

data obtained under symmetrical and asymmetrical conditions (see Discussion). In the concentration ranges studied (0.015–1 M in symmetrical and 0.540–4 M external with 0.108 M internal in asymmetrical solutions), the normal Na^+ channel has a larger conductance than the BTX-modified channel. In symmetrical Na^+, the normal channel conductance/BTX-modified channel conductance ratio is 1.7 at 0.015 M and 2.5 at 1 M Na^+.
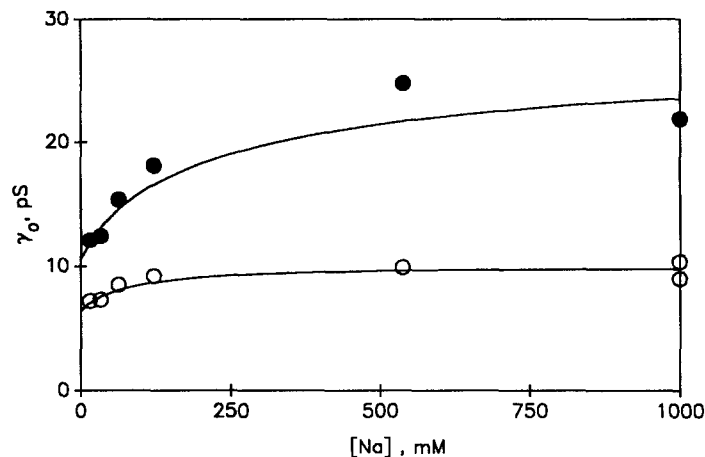

FIGURE 5. Conductance vs. $[Na^+]$. Single-channel conductance was measured at zero voltage as described in Materials and Methods at the indicated symmetrical $[Na^+]$. The solid lines are curves predicted by the 3B2S model illustrated in Fig. 8 A with the proviso that no more than one ion can be in the channel at any given time, and with surface charge densities of -0.8 e/nm^2 in the internal vestibule and -0.1 e/nm^2 in the external vestibule. The parameters of the model were obtained by fitting the complete set of I-V relations in both symmetrical and asymmetrical conditions.

Ion Selectivity

Fig. 6 A shows that the normal and the modified channels are ideally cation selective. The reversal potentials determined from the I-V relations for the two types of channels shown in Fig. 6 A are very close to that expected from the ionic composition of the aqueous solutions (4 M external/0.108 M internal), assuming that anions are impermeant. The reversal potential was in both cases within 2 mV of the Na^+ equilibrium potential. The channel conductances obtained from the slope of the straight lines were 29.7 pS for the normal and 9.9 pS for the BTX-modified Na^+ channel. Since the currents measured are inward (i.e., from the high to the low concentration side), these conductances should approach the values expected for symmetrical 4 M Na^+. For this last case the energy barrier model (Fig. 8) predicts conductances of 24.5 and 9.74 pS for the normal and BTX-modified Na^+ channels, respectively.

The ion selectivity between Na^+ and NH_4^+ was determined by measuring the reversal potential under bi-ionic conditions (Fig. 6 B). In this case the external
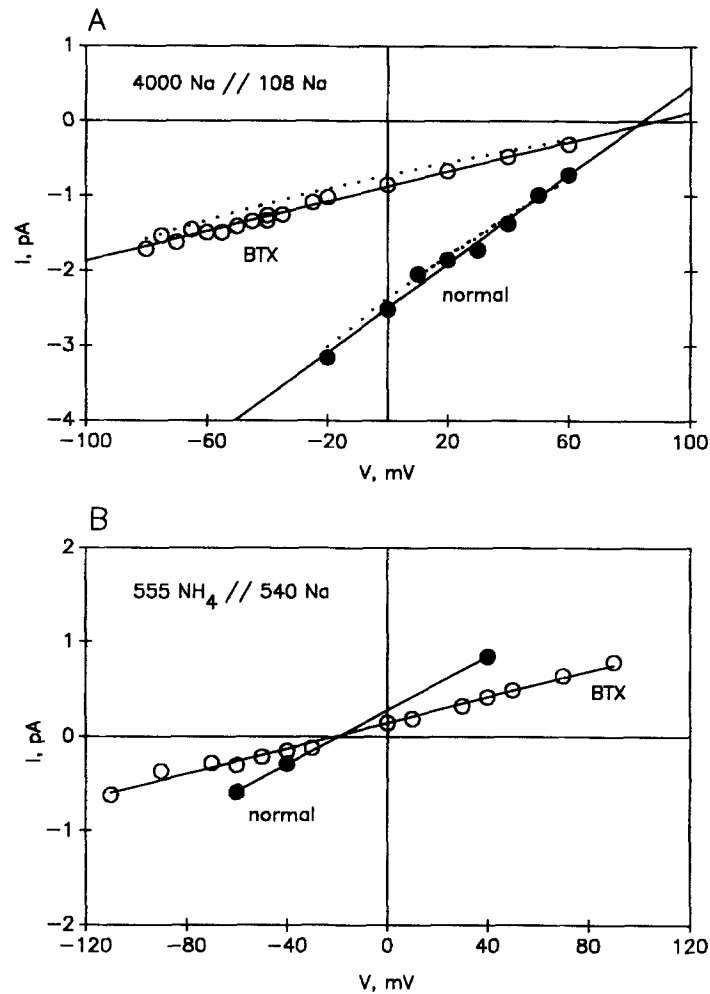
FIGURE 6. (A) I-V relationships of normal and BTX-modified channels in asymmetrical solutions. The experiment was done in extracellular 4 M Na^+ and intracellular 0.108 M Na^+. The reversal potentials, estimated from a linear regression analysis of the currents (*solid lines*), were 84.2 mV for the normal channel and 88.4 mV for the BTX-modified channel. For this Na^+ gradient the expected equilibrium potential is 86.7 mV. The dotted lines are the corresponding I-V relations predicted by the 3B2S one-ion model described in Fig. 8A with charged vestibules. (B) Selectivity to NH_4^+ of normal and BTX-modified channels. The external solution was 555 mM NH_4^+ and the internal solution contained 540 mM Na^+. The estimated reversal potentials were very similar: −19.14 and −20.90 mV for normal and BTX-modified channels, respectively.

solution contained 555 mM NH_4^+ and the internal solution contained 540 mM Na^+. The reversal potentials obtained for normal and modified channels were similar, −19.1 and −20.9 mV, respectively, and gave $P_{Na}/P_{NH_4} = 2.7$ for the normal and 2.9 for the BTX-treated channels, after appropriate compensation for liquid junction

potentials. For the squid giant axon Na$^+$ currents, a value of 3.7 was reported by Binstock and Lecar (1969) and a value of 1.75–2 was reported by Begenisich and Cahalan (1980a) using these same conditions (i.e., NH$_4$ outside and Na inside).

Temperature Dependence of the BTX-modified Channel Conductance

Fig. 7 shows the effect of temperature on the conductance of the BTX-modified channel in the form of an Arrhenius plot. A linear fit to the data gave an enthalpic change of 6.25 kcal/mol, and in the temperature range between 5 and 15°C the Q_{10} was 1.53. This last value is slightly higher than that obtained for the conductance of unmodified channels by Horn et al. (1984) (Q_{10} = 1.35) for single Na$^+$ channels in GH$_3$ cells, but is in the range (1.3–1.5) of those experimentally observed in axons (Hodgkin et al., 1952; Frankenhauser and Moore, 1963; Schauf, 1973). The enthalpy change of 6.25 kcal/mol, equivalent to 11.3 kT, obtained at −60 mV for the conductance of the BTX-modified channel, is similar to the difference in free energy for an ion in transit across the central barrier from the outermost well, 13.4 kT in
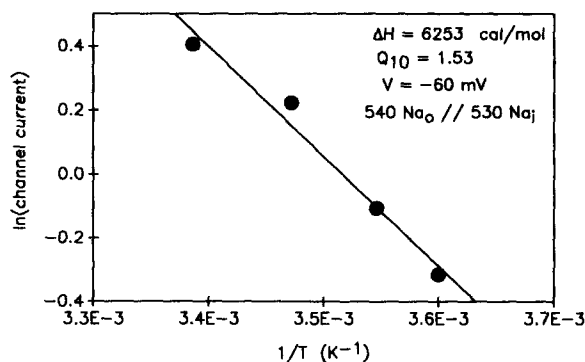

FIGURE 7. Effect of temperature on the single-channel BTX-modified conductance. The figure shows the natural logarithm of channel currents at −60 mV at four different temperatures plotted vs. 1/T (Arrhenius plot). The solid line is a linear regression of the data. From the slope of this line an enthalpic change of 6.25 kcal/mol was obtained, which is equivalent to a Q_{10} of 1.53 in the temperature range of 5–15°C.

BTX; the free energy values result from the fit of the model to the conductance data, assuming a transmission coefficient of 1. The difference may reveal a small negative entropy change for ion conduction; the uncertainties of the fit, however, do not warrant this as a firm conclusion.

DISCUSSION

BTX has been extensively used in the study of the properties of Na$^+$ channels. However, the question regarding the changes promoted by this toxin in the ion conduction properties of the channel has not been addressed in detail until now, mainly because of the lack of a suitable preparation in which to compare normal and toxin-modified channels. We present here a study of the Na$^+$-binding characteristics of normal and BTX-modified squid Na$^+$ channels under the simplest ionic conditions possible.

It is clear that one of the changes promoted by BTX is a reduction in channel conductance at all the Na^+ concentrations tested. Quandt and Narahashi (1982) and Huang et al. (1984) have reported decreased channel conductances upon treatment of neuroblastoma cells with BTX. Their experiments were done in similar ionic conditions, physiological Na^+, except for different external $[Ca^{2+}]$. The conductance with BTX was higher (10 pS as opposed to 2 pS) in lower external Ca^{2+}. In bilayers, on the other hand, the conductances reported for various BTX-treated channels range between 16 and 30 pS. The variation is generally attributed to the differences in the ionic conditions used. The higher conductance values, compared with those reported for neuroblastoma cells, could be due in part to the lower Ca^{2+} concentrations (tenths of millimolar) used in the bilayer work. External Ca^{2+} is known to block Na^+ channels in a voltage-dependent manner (Taylor et al., 1976; Yamamoto et al., 1984; Worley et al., 1986; Behrens et al., 1989). In the squid giant axon, in particular, it reduces the conductance of the unmodified channel from 14–16 pS at 4°C in the absence of Ca^{2+} to 4–6 pS in regular (sea water) concentrations (Levis et al., 1984; Llano and Bezanilla, 1984). Other evidence comes from the work with purified, reconstituted eel Na^+ channels, where removal of inactivation by limited proteolysis yields channels with higher conductances than the same preparations of channels after BTX treatment (Shenkel et al., 1989). The reduction we see in the single-channel conductance after treatment with BTX is thus consistent with observations done in other systems, although direct comparisons are restricted because of the difference in the ionic composition of the solutions, including the use of divalents.

Using symmetrical solutions we found that the single-channel conductance for both normal and modified channels is a saturating function of $[Na^+]$, but cannot be fitted by a simple Langmuir isotherm. Saturating conductance–concentration relationships are expected from a variety of ion conduction models in which the channel can accommodate from one to a limited number of ions in its conducting system (e.g., Hille, 1975; Begenisich and Cahalan, 1980a). Begenisich and Cahalan (1980a, b) described a 3B2S model that closely reproduced their results in the squid giant axon in asymmetrical salts at constant ionic strength. Their model allowed for double occupancy to account for the concentration-dependent effects on ion selectivity found in the squid Na^+ channels. In our case the departure from a Michaelis-Menten behavior (one-ion pore case) could arise purely from the presence of charges in the vestibules of the channel. For example, Green et al. (1987) found that a one-ion pore model (Lauger, 1973) that includes fixed negative charge in the vestibules can account for the conductance–$[Na^+]$ behavior of canine brain BTX-modified Na^+ channels. We have, however, maintained the 3B2S model in keeping with the previous findings in this same preparation, the squid giant axon.

Channel Conductance, Surface Charge, and Barrier Models

Fig. 8 B shows the log (conductance) vs. log $[Na^+]$ curves generated by a 3B2S model, (one-ion pore; Fig. 8 A) when the vestibules do not have a negative charge (dashed line) or when a fixed charge is included (solid line). The model curves were generated independently with the parameters fitted to all the data from the I-V relationships measured experimentally, which included symmetrical concentrations (15, 33, 63,
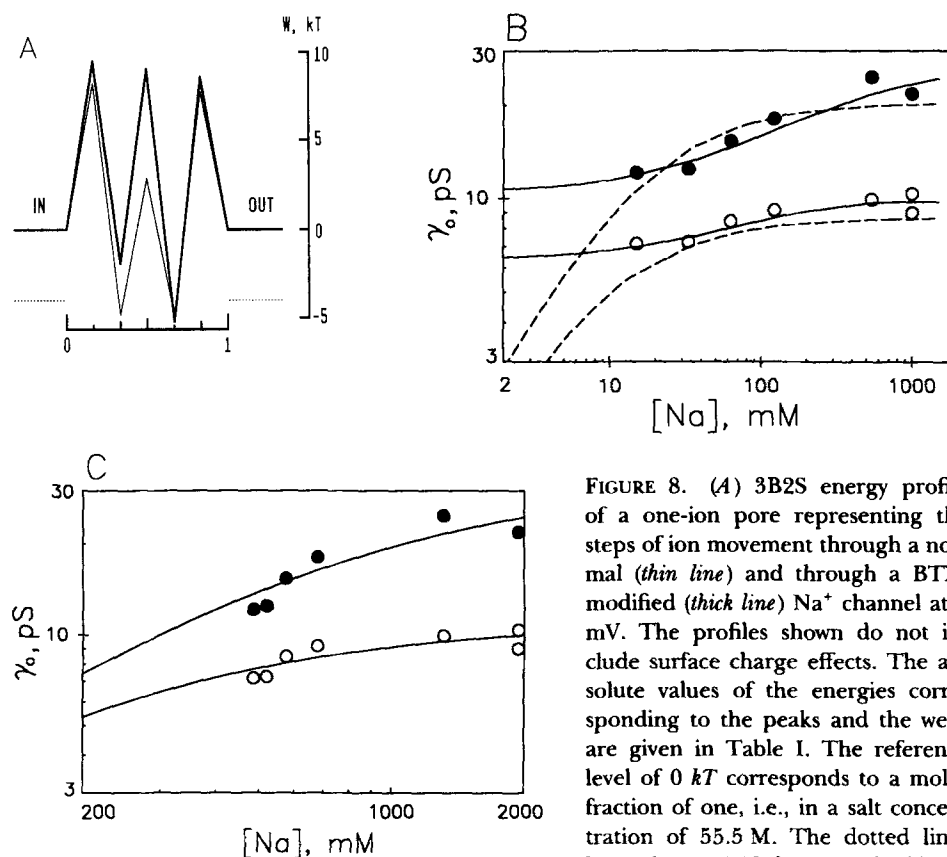
FIGURE 8. (*A*) 3B2S energy profile of a one-ion pore representing the steps of ion movement through a normal (*thin line*) and through a BTX-modified (*thick line*) Na⁺ channel at 0 mV. The profiles shown do not include surface charge effects. The absolute values of the energies corresponding to the peaks and the wells are given in Table I. The reference level of 0 kT corresponds to a molar fraction of one, i.e., in a salt concentration of 55.5 M. The dotted lines located at -4.02 kT at each side of the profile represent the reference level for a 1 M salt solution. The major difference between the two profiles is in the height of the center peak. Both this peak and the inner well were significantly raised by BTX modification. The abscissa is given in fractional electrical distance. This model was used to predict the I-V curves in Figs. 4 and 6A, and the conductance vs. concentration curves in part B of this figure (*solid lines*) and in Fig. 5, after the incorporation of surface charge effect. (*B*) Double logarithmic plot of conductance vs. the bulk [Na⁺] for normal (*filled circles*) and BTX-modified (*open circles*) Na⁺ channels. The solid lines are the conductance vs. concentration relations predicted by the hypothetical barrier model given in A and includes a surface potential at the channel entrances (see text). These curves are identical to those plotted in linear form in Fig. 5. Broken lines correspond to the predicted curves when the data were fitted with uncharged vestibules. Although the plotted conductances were determined in symmetrical solutions of the given concentrations, each curve is the result of an independent fit to all the I-V data, which also include determinations in asymmetrical Na⁺ solutions. These relations are for single-ion occupancy. (*C*) Conductance vs. [Na⁺] at the pore entrances due to the surface charge effect displayed as a double log plot. A charge density of -0.25 e/nm² was used to calculate the [Na⁺] by applying Eq. 2. Note the change of scale in the abscissa compared with the plot in *B*. The curves are simple Langmuir isotherms fitted to the data obtained in symmetrical solutions. The maximal conductances and the concentrations for half-maximal conductance obtained from the fits were, respectively: 32.87 pS and 686 mM for the untreated channels, and 11.05 pS and 214 mM for the BTX-treated channels.

122, 538, and 1000 mM) and asymmetrical concentrations (inside 108 mM and outside 540 mM, 2 M, and 4 M).

In the case of the normal Na^+ channels the 3B2S model with uncharged vestibules accounts for the conductance at high ion concentrations, but fails to explain the channel conductance at low concentrations. On the other hand, the charged vestibules–3B2S model gives a reasonable fit to the data in the whole range of concentrations. For the BTX-modified channel, including a fixed charge in the barrier model improves the fit to the data at all $[Na^+]$ compared with the "uncharged" model. As predicted by the Gouy-Chapman theory, charging the vestibules makes the conductance approach a lower finite limit at very low $[Na^+]$ (see Green et al., 1987). The fit to our data is obtained with fixed charge densities of -0.8 and -0.1 e/nm^2 for the internal and external vestibules of the channel, respectively, for both normal and BTX-modified Na^+ channels (see Table I). The different values of internal and external densities of fixed charges were essential for the simultaneous fit to the data obtained in symmetrical Na^+ and that in the presence of a Na^+ gradient. If experiments done in asymmetric conditions were not considered, the best fit was obtained with a fixed charge density of -0.25 e/nm^2, equal at both sides.

TABLE I

Fitted Parameters for the 3B2S Models with Single- or Two-Ion Occupancy in Normal or BTX-modified Na^+ Channels

Ions	Condition	Peaks			Wells		Surface charge	
		1	2	3	1	2	Inside	Outside
		kT units			*kT units*		*e/nm²*	
2	Normal	7.96	7.13	6.97	−5.50	−4.51	−0.49	−0.07
2	BTX	9.29	8.04	7.77	−4.23	−5.62	−0.49	−0.07
1	Normal	8.26	2.9	7.74	−4.79	−4.80	−0.8	−0.1
1	BTX	9.41	9.00	8.57	−1.87	−5.18	−0.8	−0.1

Energy levels are referred to a molar fraction of 1 in the bulk solution. Peaks and wells are numbered from inside to outside.

Given the limited data we have at present, we have chosen a one-ion pore model to discuss our data, but we do not exclude the possibility of multiple Na^+ occupancy. Moreover, allowing double occupancy of the channel somewhat improves the fit to the data obtained in the presence of a Na^+ gradient (e.g., Fig. 6A). Allowing the simultaneous presence of two ions in the channel also results in an increase of the maximum conductance (for a discussion on this point see Latorre and Alvarez, 1988). A two-ion 3B2S model with the energy parameters shown in Table I also represents the data adequately. Notice that the two-ion 3B2S model predicts a smaller internal surface charge density than the one-ion pore model. Regardless of the state of ion occupancy, however, fixed surface charge is essential to fit the conductance–concentration data.

The first well-developed model of ion conduction through Na^+ channels was a one-ion pore (Hille, 1975). This model has also been used more recently to describe the block of brain BTX-modified Na^+ channels by both internal and external Ca^{2+} (French et al., 1986b), and to explain conflicting results regarding the asymmetry of

ion selectivity of muscle BTX-modified channels (Garber, 1988; see below). As mentioned above, the evidence that unmodified squid Na$^+$ channels are in fact multi-ion pores comes from the work of Begenisich and Cahalan (1980a, b). They showed that the permeability ratio between NH$_4^+$ and Na$^+$ is concentration dependent when the internal [NH$_4^+$] is varied. An ion channel that can be occupied by a single ion at a time must show concentration-independent permeability ratios (e.g., Coronado et al., 1980). Other important results regarding the degree of occupancy of squid Na$^+$ channels are those of Begenisich and Busath (1981) and Busath and Begenisich (1982). Begenisich and Busath (1981) showed that the Na$^+$ flux ratio exponent is about unity and is independent of voltage in a 50-mV range. This observation suggests that in a wide range of concentrations Na$^+$ channels are empty or have at most one ion in their conductive machinery. This is not incompatible, however, with a multi-ion pore. Scarce occupancy of the channel may explain why the fit to the conductance vs. [Na$^+$] curves using a single-ion pore model is reasonably good and appropriate to explain our data. Also, through measurements of unidirectional flux ratios under bi-ionic conditions, Busath and Begenisich (1982) found flux ratio exponents greater than unity (an average of 1.15 was obtained in external Na and internal potassium). The 3B2S multi-occupancy model predicted similar higher values for the flux ratio exponents. But, as pointed out by the authors, some single-ion occupancy models can also predict flux ratio exponents other than unity in bi-ionic conditions.

In the study of BTX-modified Na$^+$ channels incorporated into planar lipid bilayers as reported by Moczydlowski et al. (1984), it came as a surprise that the affinity of the channel for Na$^+$ was much larger (K_d = 8 mM) than the one obtained for the squid Na$^+$ channel (K_d = 0.4–1 M; Begenisich and Cahalan, 1980b; Yamamoto et al., 1985) and for the frog node Na$^+$ channel (K_d = 0.368 M; Hille, 1975). Relatively high affinities have also been found in rat brain and squid optic nerve BTX-modified Na$^+$ channels (French et al., 1986a; Behrens et al., 1989). The barrier model we have used here indicates that normal and BTX-modified channels should have K_d's of the order of 458 and 314 mM (the deepest well for the BTX-modified channel is $-1.16\,kT$ and for the normal channel, $-0.78\,kT$, when the reference state is that of a 1 M salt solution), in agreement with the macroscopic Na$^+$ current measurements done in squid axons. A test of internal consistency of the model was to plot the conductance vs [Na$^+$] at the channel entrances, product of the fixed surface charge at each side, and to fit the data using a Langmuir isotherm (Fig. 8 C). The local [Na$^+$] was calculated using Eq. 2 with a symmetrical surface charge density of $-0.25\,e/nm^2$. This would be equivalent to a plot of the raw data with a Langmuir isotherm plus surface charge (Green et al., 1987). The [Na$^+$] at which half-maximal conductances were obtained for the normal and the BTX-treated channel were 686 and 214 mM, respectively, in general agreement with the energy barrier predictions. It is important to note here that the shape of the curves in Fig. 8 C is similar to those obtained by Begenisich and Cahalan (1980b) and Yamamoto et al. (1985). The values we obtained for the normal channel (458 and 686 mM with the two methods), although smaller, are of the same order of magnitude and agree well with the values of K_m reported by Begenisich and Cahalan (1980b) in the voltage range of 25–90 mV in the squid axon. The similarity arises from having included the surface charge effects in our calcula-

tions; in their case, ion replacement to maintain the ionic strength constant and the use of divalents probably mask the effects of fixed surface charges in the mouth; thus the local concentration would be similar to the bulk concentration. Our channel conductance vs. the [Na$^+$] curve (Fig. 5) for the normal channel resembles that reported by Green et al. (1987) for the dog brain BTX-treated Na$^+$ channels incorporated into planar bilayers. They obtained a K_{Na} of 1.5 M and a maximal conductance of 45 pS. Our maximal conductances (obtained in a similar way; Fig. 8 C) were 33 pS for the normal and 11 pS for the toxin-treated channels. In contrast, the BTX-modified Na$^+$ channels from the squid optic nerve incorporated into bilayers show a simple hyperbolic conductance vs. [Na$^+$] relation with a K_m of 11 mM and a maximal conductance of 23 pS. No fixed surface charges were necessary to account for the data (Behrens et al., 1989). The reason for the discrepancies is yet to be clarified.

The surface charge densities that provided a good fit to our data ranged between 0.1 and 0.8 e/nm^2. For the canine brain BTX-modified Na$^+$ channel a value of -0.38 e/nm^2 was reported by Green et al. (1987). For the squid axon Na$^+$ channel, evidence for internal fixed negative charge in the vicinity of the pore entrance was obtained from the observed reduction of the blocking potency of mono- and divalent guanidinium ions with increases of the internal salt concentration (Smith-Maxwell and Begenisich, 1987). The surface charge density obtained by these authors was -0.4 e/nm^2, a value that is in good agreement with the one found here, given that the two methods of obtaining the fixed charge density are completely independent. It is important to note that charge in the channel vestibules or in their surroundings can work as a "pre-selectivity filter." The negative potential created by these charges will concentrate cations and repel anions, conferring on the channel a cationic selectivity (Dani, 1986).

Where Is the Fixed Charge Located?

Electrophysiological measurements cannot answer unequivocally the question of the exact location of the fixed negative charge that modulates ion conduction in squid axon Na$^+$ channels. Spatially this charge can be located in the channel-forming protein or in the phospholipids forming the lipid bilayer that surrounds the channels. The following arguments can be given in support of the fact that the fixed charge is located in the channel protein. First, in planar bilayers Na$^+$ channel conductance is not affected by changing the lipid from neutral to charged phospholipids (Green et al., 1987). This indicates that the conduction machinery of the channel is located far from the surface of the lipid bilayer. However, it can be argued that canine brain Na$^+$ channel can be substantially different from squid Na$^+$ channels. Although there are several Na$^+$ channel subtypes encoded by different mRNAs and there also seems to be pharmacological heterogeneity between Na$^+$ channels (Noda et al., 1986; Moczydlowski et al., 1987), their molecular weights and general proposed structures are not so different, suggesting that their folding in the membrane could be similar. Second, the Na$^+$ channel from frog muscle incorporated into neutral phospholipid bilayers shows a single channel conductance vs. [Na$^+$] behavior very similar to the one found in the present work (Naranjo et al., 1989). Third, chemical modifications with carboxylate group-specific reagents and acidifica-

tion of the solutions decrease Na^+ channel conductance (Hille, 1968; Sigworth and Spalding, 1980; Worley et al., 1986). Note also that sialic acid residues, present on the external side of the channel, appear not to regulate the BTX-modified Na^+ channel conductance since deglycosilated, modified channels apparently attain the same conductance as shown before the treatment with neuraminidase (Catterall, 1988).

It is puzzling, however, that no apparent fixed charge was needed to fit the conductance vs. [Na^+] relation for the BTX-modified Na^+ channel from squid optic nerve incorporated into neutral bilayers (Behrens et al., 1989). This discrepancy may reflect species differences (*Loligo pealei*, this work vs. *Sepiotheutis sepioidea*, Behrens et al. [1989]). The conduction properties of BTX-treated dog brain Na^+ channels differ from those of rat brain channels mainly in the requirement for surface fixed charge (Green et al., 1987). Also, it has been reported that the rat muscle Na^+ channel does not have an appreciable charge (Moczydlowski et al., 1984), but in toad muscle the conductance vs. concentration data require a surface charge for best fit (Naranjo et al., 1989). Other possible explanations are that the retinal nerve Na^+ channel is different from the giant axon Na^+ channel, that the extraction and isolation procedures of the retinal nerve membranes might have modified the charge, or even that for the squid Na^+ channel the fixed charge is residing in the lipids.

Differences and Similarities between Normal and BTX-modified Channels

The distinction in the conduction of Na^+ ions through normal and BTX-modified channels resides mainly in the maximum channel conductance. It is possible to account for the effect of BTX on Na^+ ion conduction using the 3B2S model. Regardless of the state of occupancy of the channel, single or double, the energy levels of all three peaks and the innermost well were raised in the presence of BTX, whereas the outermost well if anything is only slightly reduced (see Table I). The extent to which BTX modifies the energy profile is such that the main differences due to ion occupancy, i.e., interaction among the ions in transit, are masked. The model predicts similar Na-binding characteristics for both channels because the outermost wells within the ion conduction system are similar (for the one-ion pore: $-0.78\,kT$ and $-1.16\,kT$ referred to a 1 M solution, implying K_d's of 458 and 314 mM, respectively). The difference in the maximum single-channel conductance arises from the fact that Na^+ ions need to pass over larger barriers in a BTX-modified channel. The most striking dissimilarity is in the central barrier of the one-ion pore model where the difference in energies amounts to $6.1\,kT$. With double occupancy the change caused by BTX at the height of this central barrier is much smaller, $0.91\,kT$, because in this model the central barrier is much higher for the unmodified channel to account for ion repulsion within the pore.

BTX appears not to modify the fixed charge present in the neighborhood of the channel entrances. Also, BTX did not modify the cation selectivity property of the channel and did not alter the permeability ratio P_{Na}/P_{NH4} when measured under bi-ionic conditions with external NH_4^+ and internal Na^+. This finding differs from the more common observation that BTX changes the permeability ratios of most permeable cations. Although we do not have a substantiated explanation for the difference, we believe that one possible origin for the unaffected permeability ratio

could be the asymmetry and sidedness of the permeability properties of Na^+ channels (e.g., Garber, 1988). A comparison with the permeability ratio measured in internal NH_4^+ and external Na^+ would clarify this issue.

REFERENCES

Albuquerque, E. X., I. Seyama, and T. Narahashi. 1973. Characterization of batrachotoxin-induced depolarization of the squid giant axon. *Journal of Pharmacology and Experimental Therapeutics.* 184:308–314.

Begenisich, T., and D. Busath. 1981. Sodium flux ratio in voltage-clamped squid giant axons. *Journal of General Physiology.* 77:489–502.

Begenisich, T., and M. D. Cahalan. 1980a. Sodium channel permeation in squid axons. I. Reversal potential experiments. *Journal of Physiology.* 307:217–242.

Begenisich, T., and M. D. Cahalan. 1980b. Sodium channel permeation in squid axons. II. Non-independence and current-voltage relations. *Journal of Physiology.* 307:243–257.

Behrens, M. I., A. Oberhauser, F. Bezanilla, and R. Latorre. 1989. Batrachotoxin-modified sodium channels from squid optic nerve in planar bilayers. Ion conduction and gating properties. *Journal of General Physiology.* 93:23–41.

Bezanilla, F. 1985. A high capacity data recording device based on a digital audio processor and a video cassette recorder. *Biophysical Journal.* 47:437–441.

Bezanilla, F. 1987. Single sodium channels from the squid giant axon. *Biophysical Journal.* 52:1087–1090.

Bezanilla, F., and C. Vandenberg. 1990. The cut-open axon technique. *In* Squid as Experimental Animals. D. L. Gilbert, W. J. Adelman, Jr., and J. M. Arnold, Editors. Plenum Publishing Corp., New York. 153–159.

Binstock, L., and H. Lecar. 1969. Ammonium currents in the squid giant axon. *Journal of General Physiology.* 53:342–361.

Busath, D., and T. Begenisich. 1982. Unidirectional sodium and potassium fluxes through the sodium channel of squid giant axons. *Biophysical Journal.* 40:41–49.

Catterall, W. A. 1975. Activation of the action potential ionophore of culture neuroblastoma cells by veratridine and batrachotoxin. *Journal of Biological Chemistry.* 250:4053–4059.

Catterall, W. A. 1988. Structure and function of voltage-sensitive ion channels. *Science.* 242:50–61.

Cecchi, X., O. Alvarez, and D. Wolff. 1986. Characterization of a calcium-activated potassium channel from rabbit intestinal smooth muscle incorporated into planar bilayers. *Journal of Membrane Biology.* 91:11–18.

Cecchi, X., D. Wolff, O. Alvarez, and R. Latorre. 1987. Mechanisms of Cs^+ blockade in a Ca^{2+}-activated K^+ channel from smooth muscle. *Biophysical Journal* 52:707–716.

Coronado, R., R. L. Rosenberg, and C. Miller. 1980. Ionic selectivity, saturation and block in a K^+-selective channel from sarcoplasmic reticulum. *Journal of General Physiology.* 76:425–446.

Correa, A. M., and F. Bezanilla. 1988. Properties of BTX-treated single Na channels in squid axon. *Biophysical Journal.* 53:226a. (Abstr.)

Correa, A. M., F. Bezanilla, and W. S. Agnew. 1990. Voltage activation of purified eel sodium channels reconstituted into artificial liposomes. *Biochemistry.* 29:6230–6240.

Correa, A. M., R. Latorre, and F. Bezanilla. 1989. Na-dependence and temperature effects on BTX-treated sodium channels in squid axon. *Biophysical Journal* 55:403a. (Abstr.)

Dani, J. 1986. Ion-channel entrances influence permeation. Net charge, size, shape, and binding considerations. *Biophysical Journal.* 49:607–618.

Eisenman, G., and J. Dani. 1986. Characterizing the electrical behavior of an open channel via the energy profile for ion permeation: a prototype using a fluctuating barrier model for the acetylcholine receptor channel. *In* Ionic Channels in Cells and Model Systems. R. Latorre, editor. Plenum Publishing Corp., New York. 63–64.

Frankenhauser, B., and L. E. Moore. 1963. The specificity of the initial current in myelinated nerve fibres of *Xenopus laevis. Journal of Physiology.* 169:438–444.

French, R. J., J. F. Worley III, and B. K. Krueger. 1986a. From brain to bilayer: sodium channels from rat neurons incorporated into planar lipid membranes. *In* Ionic Channels in Cells and Model Systems. R. Latorre, editor. Plenum Publishing Corp., New York. 273–290.

French, R. J., J. F. Worley III, W. F. Wonderlin, and B. K. Krueger. 1986b. Three sites of calcium block in single sodium channels? *Proceedings of the 8th Annual Conference of the IEEE Engineering in Medicine and Biology Society.* 962–965.

Garber, S. 1988. Symmetry and asymmetry of permeation through toxin-modified Na$^+$ channels. *Biophysical Journal.* 54:767–776.

Garber, S., and C. Miller. 1987. Single Na$^+$ channels activated by veratridine and batrachotoxin. *Journal of General Physiology.* 89:459–480.

Green, W. N., L. B. Weiss, and O. S. Andersen. 1987. Batrachotoxin-modified sodium channels in lipid bilayers. Ion permeation and block. *Journal of General Physiology.* 89:841–872.

Hagglund, J. V., G. Eisenman, and J. P. Sanblom. 1984. Single salt behavior of a symmetrical 4-site channel with barriers at its middle and ends. *Bulletin of Mathematical Biology.* 46:41–80.

Hamill, O. P., A. Marty, E. Neher, B. Sackmann, and F. Sigworth. 1981. Improved patch clamp techniques for high resolution current recording from cells and from cell-free membrane patches. *Pflügers Archiv.* 381:85–100.

Hartshorne, R. P., B. U. Keller, J. Talvenheimo, J. A. Catterall, and M. Montal. 1985. Functional reconstitution of the purified brain sodium channel in planar lipid bilayers. *Proceedings of the National Academy of Sciences, USA.* 82:240–244.

Hille, B. 1968. Charges and potentials at the nerve surface. Divalent ions and pH. *Journal of General Physiology.* 51:221–236.

Hille, B. 1975. Ionic selectivity, saturation, and block in sodium channels. A four barrier model. *Journal of General Physiology.* 66:535–560.

Hodgkin, A. L., A. F. Huxley, and B. Katz. 1952. Measurements of current voltage relations in the membrane of the giant axon of *Loligo. Journal of Physiology.* 116:424–448.

Horn, R., C. A. Vandenberg, and K. Lange. 1984. Statistical analysis of single sodium channels. Effects of *N*-bromoacetamide. *Biophysical Journal.* 45:323–335.

Huang, L.-Y. M., W. A. Catterall, and G. Ehrenstein. 1979. Comparison of ionic selectivity of batrachotoxin-activated channels with different tetrodotoxin dissociation constants. *Journal of General Physiology.* 73:839–854.

Huang, L.-Y. M., N. Moran, and G. Ehrenstein. 1982. Batrachotoxin modifies the gating kinetics of sodium channels in internally perfused neuroblastoma cells. *Proceedings of the National Academy of Sciences, USA.* 79:2082–2085.

Huang, L.-Y. M., N. Moran, and G. Ehrenstein. 1984. Gating of batrachotoxin-modified sodium channels in neuroblastoma cells determined from single-channel measurements. *Biophysical Journal.* 45:313–322.

Khodorov, B. I. 1985. Batrachotoxin as a tool to study voltage sensitive sodium channels of excitable membranes. *Progress in Biophysics and Molecular Biology.* 45:57–148.

Khodorov, B. I., and S. V. Revenko. 1979. Further analysis of the mechanisms of action of batrachotoxin on the membrane of myelinated nerve. *Neuroscience.* 4:1315–1330.

Krueger, B. K., J. F. Worley III, and R. French. 1983. Single sodium channels from rat brain incorporated into planar lipid bilayer membranes. *Nature.* 303:172–175.

Latorre, R., and O. Alvarez. 1988. Ion conduction in ion channels. Some inferences about their gross structure. *Comments on Molecular and Cellular Biophysics.* 5:193–210.

Lauger, P. 1973. Ion transport through pores: a rate theory analysis. *Biochimica et Biophysica Acta.* 311:423–441.

Levis, R. A., F. Bezanilla, and R. M. Torres. 1984. Estimate of the squid axon sodium channel conductance with improved frequency resolution. *Biophysical Journal.* 45:11a. (Abstr.)

Llano, I., and F. Bezanilla. 1984. Analysis of sodium current fluctuations in the cut-open squid giant axon. *Journal of General Physiology.* 83:133–142.

Llano, I., C. K. Webb, and F. Bezanilla. 1988. Potassium conductance of the squid giant axon. Single channel studies. *Journal of General Physiology.* 92:179–196.

McLaughlin, S. 1977. Electrostatic potentials at the membrane-solution interfaces. *Current Topics in Membrane and Transport.* 9:71–144.

Moczydlowski, E., S. Garber, and C. Miller. 1984. Batrachotoxin-activated Na^+ channels in planar bilayers. Competition of tetrodotoxin block by Na^+. *Journal of General Physiology.* 84:665–686.

Moczydlowski, E., A. Uehara, G. Xiaotao, and J. Heiny. 1987. Isochannels and blocking modes of voltage-dependent sodium channels. *Annals of the New York Academy of Sciences.* 479:269–292.

Naranjo, D., O. Alvarez, and R. Latorre. 1989. Ion conduction characteristics of batrachotoxin-modified channels from frog muscle. *Biophysical Journal.* 55:402a. (Abstr.)

Noda, M., T. Ikeda, T. Kayano, H. Suzuki, H. Takeshima, M. Kurasaki, H. Takahasi, and S. Numa. 1986. Existence of distinct sodium channel messenger RNA's in rat brain. *Nature.* 320:188–192.

Quandt, F. N., and T. Narahashi. 1982. Modification of single Na^+ channels by batrachotoxin. *Proceedings of the National Academy of Sciences, USA.* 79:6732–6736.

Recio-Pinto, E., D. S. Duch, S. R. Levinson, and B. W. Urban. 1987. Purified and unpurified sodium channels from electroplax in planar lipid bilayers. *Journal of General Physiology.* 90:375–395.

Rosenberg, R. L., S. A. Tomiko, and W. S. Agnew. 1984. Reconstitution of neurotoxin-modulated ion transport by the voltage-regulated sodium channel isolated from the electroplax of the *Electrophorus electricus. Proceedings of National Academy of Sciences, USA.* 81:1239–1243.

Schauf, C. L. 1973. Temperature dependence of ionic currents kinetics of *Myxicola* giant axons. *Journal of Physiology.* 235:197–205.

Shenkel, S., E. C. Cooper, W. James, W. S. Agnew, and F. J. Sigworth. 1989. Purified, modified eel sodium channels are active in planar bilayers in the absence of activating neurotoxins. *Proceedings of the National Academy of Sciences, USA* 86:9592–9596.

Sigworth, F. J., and B. C. Spalding. 1980. Chemical modification reduces the conductance of sodium channels in nerve. *Nature.* 283:293–295.

Smith-Maxwell, C., and T. Begenisich. 1987. Guanidinium analogues as probes of the squid axon sodium pore. Evidence for internal surface charges. *Journal of General Physiology.* 90:361–374.

Taylor, R. E., C. M. Armstrong, and F. Bezanilla. 1976. Block of sodium channels by external calcium ions. *Biophysical Journal.* 16:27a. (Abstr.)

Vandenberg, C., and F. Bezanilla. 1988. Single-channel, macroscopic and gating currents from Na channels in squid giant axon. *Biophysical Journal.* 53:226a. (Abstr.)

Villarroel, A. 1989. Mechanism of ion conduction in the large calcium-activated potassium channel. Ph. D. dissertation. University of California. Los Angeles, CA. 133 pp.

Villarroel, A., and G. Eisenman. 1987. Surface charge in a barrier model can explain the low concentration I-V behavior of the Ca^{2+}-activated K^+ channel. *Biophysical Journal.* 51:546a. (Abstr.)

Worley, J. F., R. J. French, and B. K. Krueger. 1986. Trimethyloxonium modification of single batrachotoxin-activated sodium channels in planar bilayers. Changes in unit conductance and in block by saxitoxin and calcium. *Journal of General Physiology.* 87:327–349.

Yamamoto, D., J. Z. Yeh, and T. Narahashi. 1984. Voltage-dependent calcium block of normal and tetramethrin-modified single sodium channel. *Biophysical Journal.* 45:337–343.

Yamamoto, D., J. Z. Yeh, and T. Narahashi. 1985. Interactions of permanent cations with sodium channels of squid axon membranes. *Biophysical Journal.* 48:361–368.